

**GEOLOGICAL EVOLUTION OF THE LARGEST SHIELD VOLCANO BEARING MARE OF THE MOON, MARE TRANQUILLITATIS: BASED ON DETAILED MORPHOLOGICAL, MINERALOGICAL, TOPOGRAPHIC STUDIES USING MULTIPLE DATA SETS.** Henal Bhatt<sup>1</sup>, P. Chauhan<sup>2</sup>, Paras Solanki<sup>1</sup>, <sup>1</sup>M. G. Science Institute, Ahmedabad 380009, India, <sup>2</sup>Indian Institute of Remote Sensing, (ISRO), Dehradun, Uttarakhand, India. ([henalbhatt@yahoo.in](mailto:henalbhatt@yahoo.in))

**Introduction:** In this work, we have analysed the irregular shaped Mare Tranquillitatis based on its morphology, mineralogy and topography to understand its geological evolution in the Lunar formation history. This area is very unique as it resides the largest shield volcano of the Moon, compared to all the other circular mare basins at the near side of the Moon. It is located towards eastern near side at 7°N, 30°E and is a Pre-Nectarian age basin [1]. It is well known for Apollo 11 landing site and it shows characteristic two basin ring structure [2], with diameter of 800 km from east to west.

**Data sets used:** Data from Moon Mineralogy Mapper (M<sup>3</sup>) instrument [3], [4] on-board Chandrayaan-1 have been used to study composition and basalt emplacement history of the area. M<sup>3</sup> Level-2 data product of OP1A and OP1B optical period which contains pixel located, thermally corrected, photometrically corrected, reflectance data is acquired [5], [6]. To study the topography of the area, Lunar Orbiter Laser Altimeter (LOLA) Digital Elevation Model (DEM) data of 1024 pixel/degree resolution from Lunar Reconnaissance Orbiter (LRO) mission was acquired from PDS Geoscience Node. To study major morphologic features of the mare, Lunar Reconnaissance Orbiter Camera (LROC) Wide Angle Camera (WAC) 100 m data of the Lunar Reconnaissance Orbiter (LRO) is used and acquired from <https://astrogeology.usgs.gov>.

**Methodology:** The mineralogical variations is studied using Integrated Band Depth (IBD) parameter technique from [7]. IBD False Colour Composite (FCC) has been prepared by assigning a red channel to IBD-1, green to IBD-2 and blue to the 1578 nm M<sup>3</sup> albedo channel (Fig. 1). The basaltic units have been delineated based on visually found colour variation in the IBD FCC (Fig. 1). From the each spectral units number of fresh small craters (~1 km diameter) were sampled to analyse spectral variability. Band parameter such as band depth, band strength, band area were calculated in Matlab for each spectral profile. The band parameters were analysed as per [8], [9], [10] to derive mineralogical abundances of the basaltic units. The morphological map was generated using LROC WAC data and all the morphological features overlaid on LOLA DEM data to understand the overall geology of the study area (Fig. 2, upper image). Some of the observations were made from GRAIL data (<https://quickmap.lroc.asu.edu>), to understand the evolution of this non-mascon mare (Fig. 3).

**Results and Discussions:** Mare Tranquillitatis is delineated in to 22 spectral units based on IBD parameter analysis (Fig. 1). The band parameters analysis was conducted as per [8], [9], [10] suggest the abundance of mafic silicate mixture, particular, mixture of olivine and medium to high calcium pyroxene bearing basaltic material in the area (Fig. 1). Details of this analysis is reported in the [11]. Graphical trends suggests that basalts of eastern shield mare would have been comparatively more pyroxene bearing compared to the basalts from western deepest part, which would have been more olivine bearing compared to the eastern shield mare basalt (Fig. 1, lower right plot) [11].

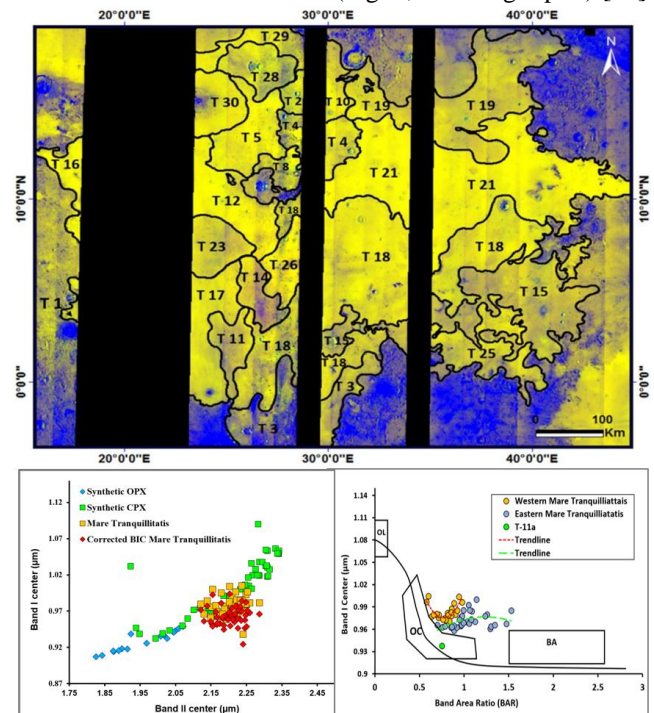


Figure 1: Upper image is M<sup>3</sup> IBD FCC, where delineated basaltic units are marked with black boundaries. Lower left graph is BI vs. BII center plot, presents calcic pyroxene bearing basaltic material and lower right graph is BI center vs. BAR plot shows olivine and calcic pyroxene mixture for MT.

This region resides more than 50% of the total Irregular Mare patches [12], [13], which are the recent volcanic features, indicates that this region has been stayed volcanically active for the longest period in the lunar geological timescale. Eastern and western region of this mare shows significant variation in topography (~2 km) and morphology, as the eastern part resides Cauchy shield volcano. The eastern part shows the largest spatially distributed basaltic units, which shows longest volcanic

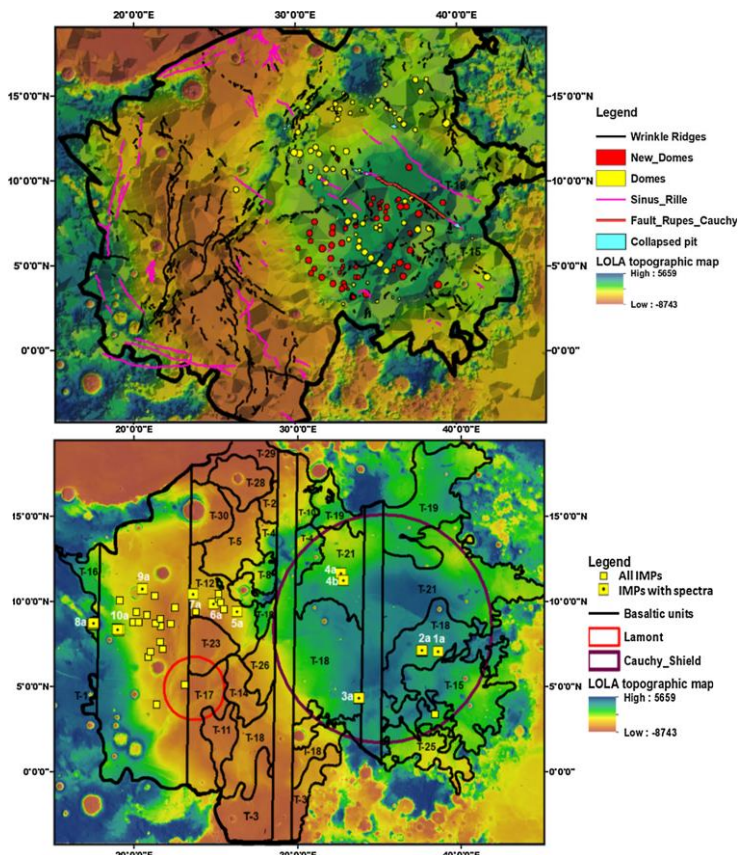


Figure 2: Both the image shows colour coded LOLA topographic map. Upper image is overlaid by all the morphological features present in the area. Lower image overlaid by all the basaltic units and IMPs.

flows units (T-18, T-21 unit, Fig-2) around the volcano. Western part shows smaller spatial distribution of basaltic units. This mare comprises variety of the morphological and structural features such as Wrinkle ridges, Sinus rille, Domes, Fault and Collapsed pit. In Fig. 2 blue region shows Cauchy shield (non-mascon) region which is elevated compare to western Lamont region (mascon) region shows topographic low of -5 km. We identified 61 new domes (red circles, Fig. 2-upper image) in the shield plateau region over to previously identified dome (marked yellow circles, Fig. 2-upper image) by other workers. This investigation indicates that area have been tectonically active up to longer period after shield formation. The ridge system in MT yields an average formation time of 2.4 Ga, which is 1.4 Ga after its oldest surface lavas, which spanned for significantly longer period than for any other basin [14]. This indicates longest period for tectonic settlement. GRAIL observation clearly shows that non-mascon Cauchy shield (yellow circle, Fig. 3) located on a unique geometrical triangular centroid, made by all the circular mascon basin (Fig. 3). This observation gives the most accurate reason for the formation of shield volcano on Moon. We interpret that all the circular impact basins-Mare Imbrium, Mare Serenitatis, Mare Crisium, Mare Smythi, Mare Nectaris made a pressure induced centroid beneath the surface, where the magmatic cumulate zone of greater size may have formed and erupted on the surface with time to make the Cauchy shield. The results are in

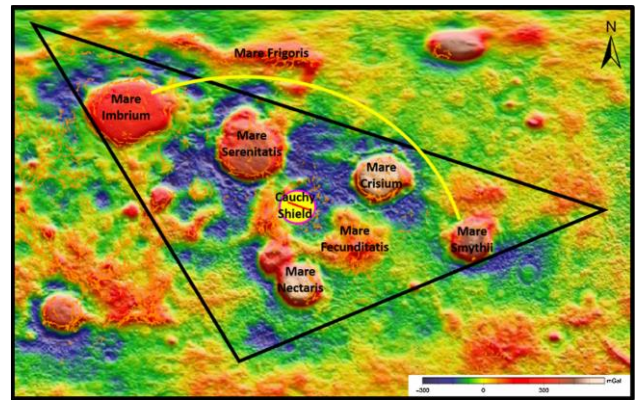


Figure 3: GRAIL Bouguer gravity anomaly map marked with geometric triangular centroid (yellow circle-Cauchy shield) of MT.

agreement with the previous works [15], [16], which suggest that mantle upliftment would not have played any role for the formation of the Cauchy shield. This work suggests that Cauchy shield may have formed due to high pressure and stresses generated at the centroid by all the surrounded eastern mare basins, marked by triangle in the Fig. 3. The Lamont region is the frozen remnant of the regional magmatic plumbing system that runs from Oceanus procellarum to north at mare frigoris and comes down to western part of mare Tranquillitatis [17]. Detailed justification for these all findings can be found at [11].

**Conclusion:** This study indicates that Mare Tranquillitatis has staid volcanically and tectonically more active for the longest period in the lunar history. Cauchy shield volcano shows longest and largest basaltic flow units compare to other parts of the mare. Detailed mineralogical, morphological, topographic study of Mare Tranquillitatis suggest that eastern half and western part of mare shows different geologic parameters like mineralogy, morphology and topography. Cauchy volcano is located on the triangular centroid made by surrounding impact basins, which produced stress induced zone beneath the centroid, subsequently large cumulative magmatic zone and eruption of the volcano at the eastern region of mare. This study indicates the most possible reason for the formation of the largest shield volcano on this one plate planetary body-the Moon.

**References:** [1] Wilhelms D. E. (1987) *JGR*, 105, 29,239-29,275 [2] De Hon R. A. (2017) *LPSC XLVIII*, abstract #2769. [3] Goswami J. N. and Annadurai M. (2009) *Curr. Sci.*, 96, 486-491. [4] Boardman J. W. et al. (2011) *JGR*, 116(E6). [5] Clark R. N. et al. (2011) *JGR*, 116(E6). [6] Besse S et al (2013) *Icarus*, 222(1), 229-242. [7] Mustard J. F. et al (2011), *JGR*, 116, E00G12. [8] Klima R. L. et al. (2011) *MPS*, 46(3), 379-395. [9] Gaffey M. J., et al. (1993) *Icarus*, 106(2), 573-602. [10] Cloutis E A et al., (1986), *JGR*, 91(B11), 11641-11653. [11] Bhatt H. et al. (2020) *JESS*, 129(45). [12] Barden S. E. et al. (2014) *Nature Geoscience*, 7(11), 787. [13] Bhatt H. (2020) *LPSC*, abstract #1533. [14] Li B. et al. (2018) *JSG*, 109, 27-37. [15] Zuber M. T. et al. (2013), *Science*, 339(6120), 668-671. [16] Tye A. and Head J. W. (2013), *LPSC*, abstract #1319. [17] Neuman G. A. et al. (2015) *Science Adv.*, 1(9), e1500852.